

# PSCAD/EMTDC 모델링에 의한 30kW급 VPL 장치의 운용 특성

호삼 살라\*, 유현상\*, 최성문\*\*, 이중선\*, 노대석\*  
\*한국기술교육대학교 전기공학과, \*\* (재)녹색에너지연구원  
e-mail:hossam\_salah@koreatech.ac.kr

## A Study on Operation Characteristics of 30kW VPL Device Based on the PSCAD/EMTDC Modeling

Hossam S. Mohamed\*, Hyun-Sang You\*, Sung-Moon Choi\*\*,  
Joong-Seon Lee\*, Dae-Seok Rho\*

\*Dept. of Electrical Engineering, Korea University of Technology and Education

\*\*Green Energy Institute

### Abstract

The rapid increase of renewable energy sources in distribution systems, such as photovoltaic systems (PV) has led to significant voltage regulation challenges, where customer voltages may violate the allowable limit (207V-233V). Conventional solutions based on the expansion of power infrastructure are often associated with high costs and long construction periods, making them less practical. Therefore, this paper presents the concept of virtual power line (VPL) device which increases the renewable hosting capacity without having to expand the physical infrastructure in distribution systems. The VPL system consists of a real-time monitoring, control platform and energy storage system (ESS). The platform collects operation data from the distribution system, renewable energy sources, and grid flexibility resources, and accordingly controls the ESS to perform charging and discharging operations. A 30[kW] VPL test system, including a simulated distribution system, photovoltaic (PV) generation system, and VPL device, is modeled using PSCAD/EMTDC. Simulation results demonstrate that the proposed VPL device effectively mitigates both over-voltage and under-voltage phenomena caused by reverse power flow and load variations. By appropriately controlling the ESS, the VPL system maintains customer voltage within the permissible range and significantly improves the hosting capacity of renewable energy.

## 1. Introduction

Recently, the rapid increase in renewable energy integration, particularly photovoltaic (PV) systems, has caused significant voltage issues in distribution systems. During daytime, the reverse power flow from PV systems may lead to over-voltage condition, while during peak load conditions, long distribution feeders with high impedance may result in under-voltage condition at customer side. These issues limit the hosting capacity of renewable energy and may require expansion of power infrastructure which is costly and require long periods. To address these challenges, this paper proposes a Virtual Power Line (VPL) device that improves hosting capacity without expanding the existing power system. The VPL system consists of a platform and an Energy

Storage System (ESS), which operates based on real-time grid conditions. A 30[kW] VPL system is modeled using PSCAD/EMTDC software, and its operation characteristics are evaluated under various voltage conditions. The results demonstrate that the proposed VPL device effectively mitigates voltage violations and enhances renewable energy hosting capacity.

## 2. Operation Characteristics of VPL

The Virtual Power Line (VPL) system is designed to enhance the hosting capacity of renewable energy sources without expanding the existing power infrastructure. It consists of a VPL platform and an Energy Storage System (ESS). The VPL platform monitors real-time operation data from the distribution system,

including voltage, current, photovoltaic (PV) output, and demand response (DR) status. Based on this information, it generates control signals for the ESS. The ESS performs charging and discharging operations to regulate voltage within the allowable range. Charging is activated during over-voltage conditions caused by reverse power flow, while discharging is used to mitigate under-voltage condition during peak load conditions. the 30[kW] VPL test system shown in Fig. 1. consists of a simulated distribution system, a PV generation system, and the VPL system. The distribution system includes low-voltage feeders and customer loads, while the PV system injects power into the distribution system through a grid-connected inverter. The VPL system interacts with both the PV system and loads to maintain voltage stability.

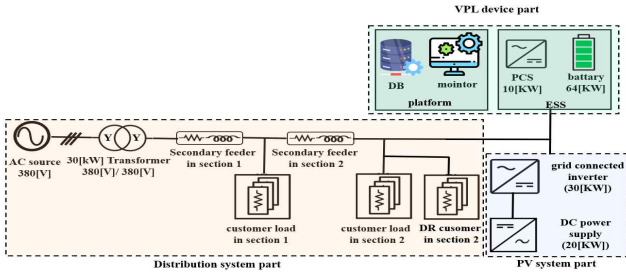


[Fig. 1] 30[kW] VPL device Configuration

### 3. Modeling of the 30kW VPL Test Device Using PSCAD/EMTDC

#### 3.1 Simulated Distribution System

The simulated distribution system shown in Fig. 2. consists of a 3 phase, 4 wire 380[V] AC source, distribution transformer with a capacity of 30[kVA], and a low-voltage feeder. The feeder is modeled using multiple sections composed of resistance and reactance to represent voltage drop characteristics. Customer loads, including general loads and demand response (DR) loads, are connected at different points along the feeder to analyze voltage variations under various operating conditions.

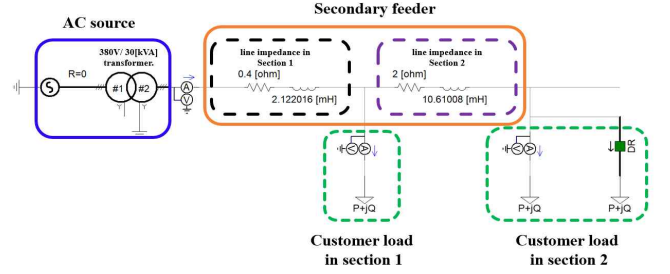


[Fig. 2] Simulated distribution system modeling

#### 3.2 Simulated Photovoltaic (PV) System

The simulated photovoltaic (PV) system shown in Fig. 3. consists of an equivalent PV array and a grid connected inverter. The PV array is modeled as an aggregated DC source representing multiple PV modules. The inverter is implemented using a current control scheme in the d-q reference frame, enabling independent control of active and reactive power through a decoupling method. The control algorithm of the PV inverter is described by Eq. (1) and Eq. (2).

$$V_d = (I_{ref-d} - I_d) \cdot (K_p + \frac{K_i}{s}) - I_q \cdot \omega L + V_{sq} \quad (1)$$

$$V_q = (I_{ref-q} - I_q) \cdot (K_p + \frac{K_i}{s}) + I_d \cdot \omega L \quad (2)$$

Where,  $V_d, V_q$  : output voltage of d-q axis,  $I_{ref-dq}$  : reference current of inverter in d-q axis,  $I_d, I_q$  : output current of d-q axis,  $V_{sq}$  : instantaneous voltage of output terminal,  $K_p$  : proportional gain,  $K_i$  : integral gain.

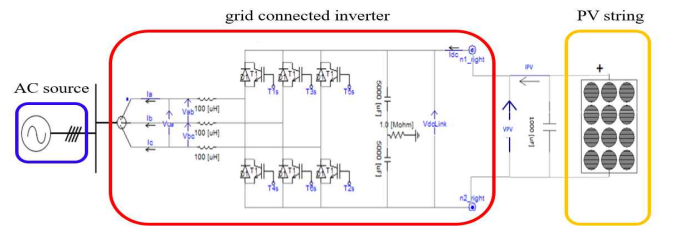


[Fig. 3] modeling of Simulated PV system

#### 3.3 VPL System

##### 3.3.1 VPL oriented ESS

The VPL ESS consists of a battery and a power conditioning system (PCS). The battery is modeled using an equivalent circuit considering state of charge (SOC), internal resistance, and voltage characteristics. the battery voltage is determined based on the relationship between the electromotive force and internal resistance,

as described by Eq. (3) ~ Eq. (5).

$$E_{bat}(t) = E_0 - K \frac{1}{SOC} + A \exp(-BQ(1 - SOC))$$

$$(3) SOC = \frac{Q - \int_{t_0}^{t_1} I_{bat}(t) dt}{Q} \times 100$$

$$(4) V_{bat}(t) = E_{bat}(t) - I_{bat}(t) \cdot R_{bat} \quad (5)$$

Where,  $E_{bat}(t)$ : electromotive force[V],  $E_0$ : battery constant voltage[V],  $K$ : polarization voltage[V],  $Q$ : battery capacity [Ah],  $A$ : exponential zone amplitude[V],  $B$ : exponential zone time constant inverse[1/Ah],  $SOC$ : state of charge[%],  $V_{bat}(t)$ : battery voltage[V],  $I_{bat}(t)$ : battery current[A],  $R_{bat}(t)$ : battery internal resistance [ $\Omega$ ]. The PCS enables bidirectional power flow between the ESS and the distribution system and regulates active and reactive power based on reference currents, which are shown in Fig. 4. and defined by Eq. (6) and Eq. (7).

$$I_{d,ess}^* = (K_p + \frac{K_i}{s})(P_d^* - P_d(t)) \quad (6)$$

$$I_{q,ess}^* = (K_p + \frac{K_i}{s})(Q_q^* - Q_q(t)) \quad (7)$$

where,  $I_{d,ess}^*$ : d component of reference current of ESS,  $P_d^*$ : d component of reference active power of ESS,  $P_d(t)$ : d component of reference actual active power,  $I_{q,ess}^*$ : q component of actual current,  $Q_q^*$ : q component of reference reactive power,  $Q_q(t)$ : q component of actual reactive power.

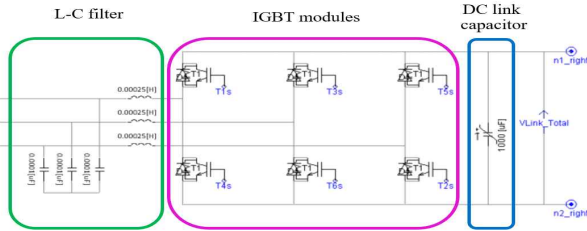


[Fig. 4] Modeling of PCS for ESS

### 3.3.2 VPL Platform

The VPL platform shown in Fig. 5 monitors real-time operation data, including voltage, current, PV output, and load conditions. Based on this information, it determines the appropriate operation of the ESS. When the customer voltage exceeds the allowable range, the ESS operates in charging mode, while during

under-voltage conditions, it operates in discharging mode. the control logic operation is defined by Eq. (8).

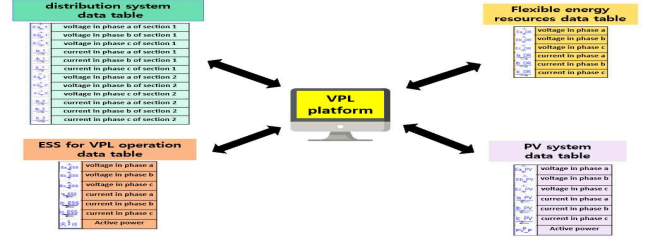


[Fig. 5] Modeling of monitoring device

$$\delta(t) = \begin{cases} -1 & \text{if } V_{cuts}(t) > V_{uplim} \\ 1 & \text{if } V_{cuts}(t) < V_{lowlim} \end{cases} \quad (8)$$

Where,  $\delta(t)$ : ESS for VPL operation mode,  $V_{cuts}(t)$ : customer voltage[V],  $V_{uplim}(t)$ : allowable upper limit of customer voltage[V],  $V_{lowlim}(t)$ : allowable lower limit of customer voltage[V].

### 3.4 Overall System

The overall configuration of the 30[kW] VPL test system shown in Fig. 6 integrates the distribution system, PV system, and VPL system. The coordinated operation of these components enables effective voltage regulation and improved hosting capacity of renewable energy sources.

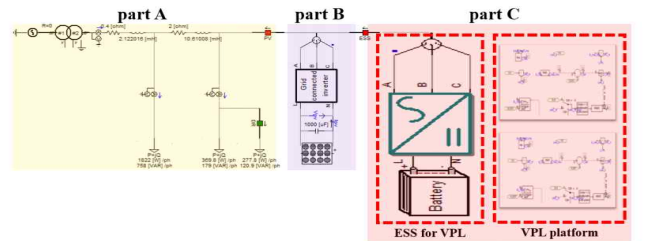


[Fig. 6] Modeling of Entire system

## 4. Case Studies

### 4.1 Simulation Conditions

The simulation is conducted on a 30[kW] VPL test system using PSCAD/EMTDC. The distribution feeder is modeled with two sections to reflect voltage variations along the line. The PV system capacity is set to 15 kW, and different load conditions are considered to analyze both over-voltage and under-voltage scenarios. The detailed parameters are summarized in Table 1.

[Table 1] Simulation Conditions

items	contents		
AC source[V]	3φ 380		
line impedance[Ω]	section 1	0.4+j0.8	
	section 2	1+j2	2+j4
3φ customer [kW]	Over-voltage	section 1	5.4
		section 2	2.2
	under-voltage	section 1	13.5
		section 2	2.3
PV system [kW]	15		
DR[kW]	0.5(20% of the peak load of customer in section 2)		

### 4.2 Operation Characteristics of VPL System under Over-voltage Phenomena

Based on the test conditions in Section 4.1, Fig. 7. illustrates the operation characteristics of the 30[kW] VPL device under customer side over-voltage phenomena. Region A represents steady-state operation before PV integration, Region B shows the voltage rise after PV connection, and Region C indicates ESS charging operation. In Fig. 7, Region A shows the customer voltages in are 215 V and 209 V. In Region B After PV integration, the voltage in Section 2 rises to 234 V due to reverse power flow, exceeding the allowable limit. In Region C, ESS charging (2kW) reduces the voltage to 232 V, maintaining it within the allowable range.

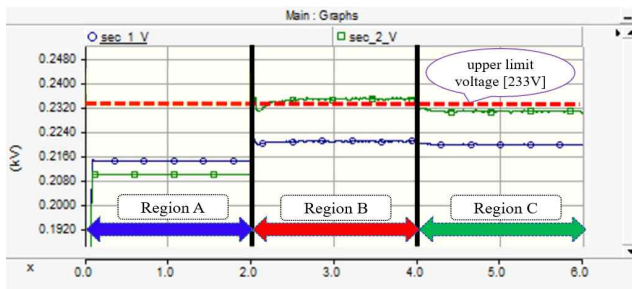


[Fig. 7] Operation characteristics of VPL device with over-voltage phenomena

### 4.3 Operation Characteristics of VPL System under Under-voltage Phenomena

Based on the test conditions in Section 4.1, Fig. 8. illustrates the operation characteristics of the 30[kW] VPL device under customer-side under-voltage phenomena. Region A represents peak load conditions, Region B shows load reduction by demand response (DR), and Region C indicates ESS discharging operation. In Fig. 8, Region A shows the customer voltages are 203

V and 201 V, indicating under-voltage phenomena. In Region B, the voltages increase to 205 V and 203 V due to DR. In Region C, ESS discharging (3kW) raises the voltages to 208 V and 210 V, restoring them within the allowable range confirming effective mitigation of under-voltage.

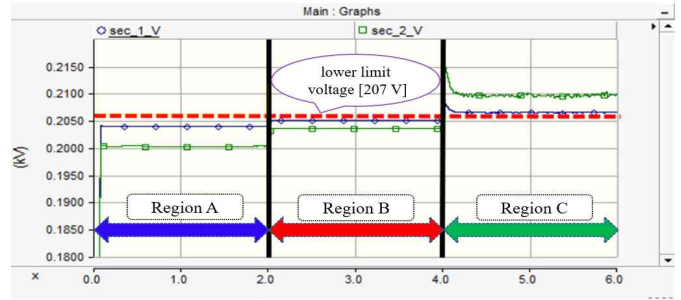


[Fig. 8] Operation characteristics of VPL device with under-voltage phenomena

## 5. Conclusions

This paper presented a 30[kW] Virtual Power Line (VPL) device as an effective solution for enhancing the hosting capacity of renewable energy sources without requiring expansion of existing power infrastructure. PSCAD/EMTDC-based model integrating a distribution system, photovoltaic (PV) system, and VPL system was developed to evaluate its operation performance. The simulation results demonstrated that the proposed VPL device effectively mitigates both over-voltage and under-voltage phenomena through coordinated charging and discharging of the Energy Storage System (ESS). In particular, the VPL device maintains customer voltage within the allowable range (207-233V) under reverse power flow and peak load conditions. Furthermore, the results indicate that the effectiveness of the VPL device becomes more significant in long feeders and high PV penetration scenarios, where voltage deviations are more severe.

### References

[1] Y. Yang et al., "Coordinated Control of Distributed Energy Storage Systems for Voltage Regulation in Distribution Networks," IEEE Transactions on Smart Grid, vol. 12, no. 4, pp. 3242-3253, Jul. 2021.